ANALYSIS OF MASONRY SHEAR WALLS USING STRUT-AND-TIES MODELS

Fonseca, Fernando S.[1] and Dillon, Patrick B.[2]

ABSTRACT

Mechanical models provide a good combination of efficiency, reliability, and practicality for most masonry analysis and design scenarios. The use of stress fields, which are based on the lower-bound theorem of the theory of plasticity, has been shown to be efficient and reliable. Stress fields have been combined with the truss analogy to produce what is known as the strut-and-tie modeling procedure. This method makes it easy to visualize complicated stress paths and enables designers of reinforced quasi-brittle materials to optimize the amount and location of the reinforcement. This article presents ongoing research that has the objective to develop strut-and-tie modeling procedures for masonry. Strut-and-tie modeling can be a practical tool for designing masonry structures, but unfortunately, there are no guiding principles for implementing the method in masonry design. The presented methodology uses the existing strut-and-tie guidelines for reinforced concrete as starting point.

KEYWORDS: *strut-and-tie model, numerical modeling, masonry structures, limit analysis, lower-bound theorem, masonry shear-wall, in-plane loading*

INTRODUCTION

There is a large and varied collection of masonry models due to the highly complex and heterogeneous nature of masonry as a structural material. While the individual masonry components can be considered isotropic at the material level, masonry assemblages—with their regularly repeating pattern of joints and voids—is anisotropic at the structural level. These properties of masonry make it difficult to develop models which accurately and easily describe the material behavior for all analysis and design scenarios [1].

One analysis tool that has been shown to be efficient and reliable is the use of stress fields [2]. Stress fields are based on the lower-bound theorem of the theory of plasticity and provide a safe estimate of the ultimate strength of the material [3]. The lower-bound theorem states: provided

[1] Associate Professor, Department of Civil and Environmental Engineering, Brigham Young University, Provo, UT, 84602, USA, fonseca@byu.edu
[2] Staff Engineer II, WPD & Associates Consulting Engineers, Inc., 335 Greenbrier Drive, Charlottesville, VA, 22901, pdillon@wdpa.com

that the stress fields satisfy the boundary conditions, are in equilibrium, and do not violate the yield criterion of the material, then the predicted strength is a lower bound for the ultimate strength of the material [4]. Stress fields have been combined with the truss analogy to produce what is known as the strut-and-tie modeling procedure [5]-[7].

Strut-and-tie modeling is an analysis and design technique that reduces complicated structural members to an equivalent truss assemblage, such as that shown in Figure 1. In the model, members are represented as compression struts, tension ties, and nodes. Struts (shaded strips in Figure 1) comprise sections of concrete or masonry within the member and carry compressive forces. Ties (dashed lines in Figure 1) represent the steel reinforcement in the member and are placed within the member such that the mechanical stability of the member is maintained. Nodes are regions within the member where struts and ties meet so that forces can be transferred between them. The remaining regions within the member are assumed to not act in resisting any load [8]-[9].

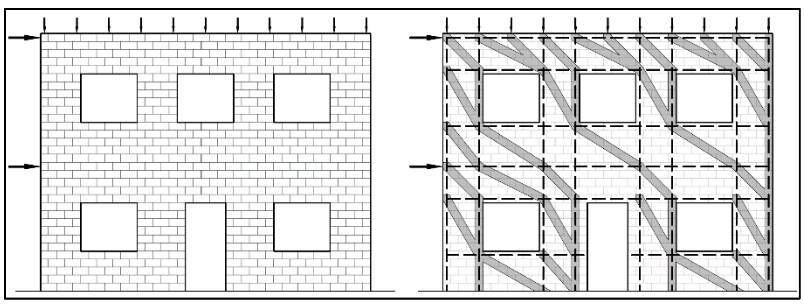

Figure 1: Strut-and-tie representation of masonry assemblage

Each strut must be sized such that its cross section is sufficient to resist the compressive loads to be transmitted. The flow of compressive forces can be idealized as three different shapes: prismatic, fan-shaped, or bottle-shaped, as shown in Figure 2. Ties must be sized and placed within the member to resist the internal tensile forces imposed by the compressive struts. Nodal regions must be sized to resist the combination of compressive forces from applied loads and the junction of struts and to provide sufficient anchorage for the reinforcing steel making up the tie [8]-[9].

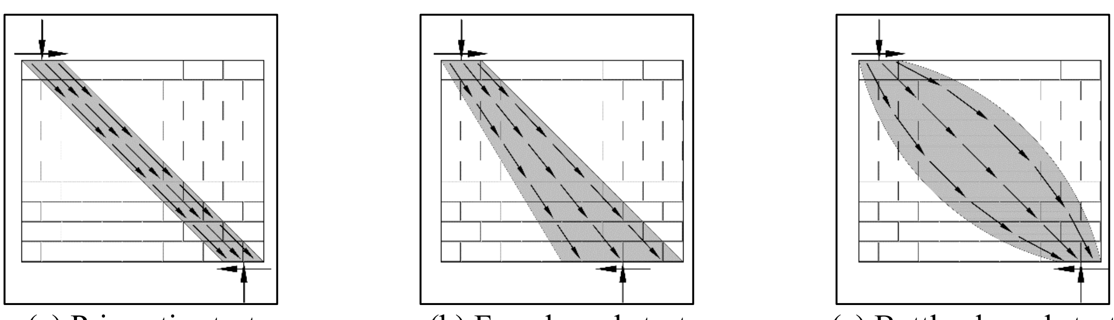

(a) Prismatic strut (b) Fan-shaped strut (c) Bottle-shaped strut

Figure 2: Strut shapes

The results of the strut-and-tie method depend on how the engineer chooses to model the member. For any member there are several strut-and-tie models that could model the stress paths within the member. The most appropriate strut-and-tie model is the one that requires the least amount of reinforcement. This is because the internal forces within the member will seek the path that minimizes the strain energy within the member. Since the reinforcement is much more deformable than the concrete or masonry, the deformation associated with the strut can be assumed to be zero. The strut-and-tie model which minimizes the area and length (i.e., total volume) of the reinforcement is the best model [7]. Since the optimal design is not always immediately apparent, implementation of the strut-and-tie method is an iterative process [9]-[11].

ACI STRUT-AND-TIE PROVISIONS

Strut-and-tie modeling is currently used for reinforced concrete structures [8]. The ACI 318 code [8] requires that struts, ties, and nodal zones be designed such that Equation 1 is satisfied.

$$\phi F_n \geq F_u \tag{1}$$

The nominal strength of struts is based on the effective compressive strength of the concrete multiplied by the smallest cross-section of the strut. The code also provides factors for reducing the effective compressive strength of struts for several reasons, e.g., the strut shape. No reduction is required for struts that are prismatic, but a reduction is needed for fan-shaped or bottle-shaped struts. Factors are also given to reduce the effective strength of struts that are located in tensile regions of members or in areas where they are likely to be traversed diagonally by cracks. In all cases, the code permits less-stringent reductions to be used for areas meeting minimum reinforcement requirements.

The nominal strength of nodal zones is similar to that of compression struts. Nodal zones typically have three faces, one for each member that meets in the node. If more than three struts or ties intersect in a nodal zone, then the resultant forces and faces are determined by combining some of the forces together. Each face of the nodal zone is measured normal to the axis of the strut or tie, and the critical area used in design is the smallest of the three faces. The effective compressive strength of the nodal zone is reduced for nodal zones that contain ties. The code also restricts the angle at which struts and ties intersect at nodal zones to between 25 and 65 degrees.

The nominal strength of tension ties is the sum product of the tensile strength and cross section of the reinforcing bars in the tie. The concrete between and around the reinforcement does not contribute any tensile strength to the tie, but it is included because it is necessary for transferring the forces between the tie and the adjacent concrete. The tension force for each tie is assumed to act through the centroid of the reinforcement cross section. Adequate development length is needed for tension ties beginning at the point where the axis of the tie first crosses into the intersecting strut to the end of the nodal zone.

ADAPTING THE ACI 318 CODE STRUT-AND-TIE PROVISIONS FOR MASONRY

Several researchers [12]-[17] have concluded that strut-and-tie modeling is a practical tool for analysing and designing masonry shear walls. There are, however, no recommended practices or guiding principles for implementing the strut-and-tie method in masonry design. In the work presented herein, the existing guidelines of ACI 318 code [8] are used as a starting point for developing strut-and-tie modeling guidelines for masonry.

Strut-and-tie models are typically used to determine the required reinforcement amount and location within a member to resist the ultimate load demands placed on the member. This means that in a typical scenario, the loads are known and the reinforcement is unknown. In an analysis case, the reinforcement size and spacing are known and the object of the analysis is to determine the member capacity. For design scenarios, the principle of minimum strain energy states that the model with the minimum strain energy for a given strength demand is the most correct model; which means the model with the minimum volume of reinforcement for a given strength demand is the correct model. For analysis scenarios, the objective is to determine the strut-and-tie model that produces the highest predicted capacity and meets all of the modeling guidelines.

Specimens and Analyses

The current study constructed strut-and-tie models for the fully grouted specimens presented by Voon [18]. Each specimen was initially modeled using the strut-and-tie methodology prescribed in the ACI 318 code [8]. The base compression strength f'_m of the masonry struts and nodal regions was assumed to be the strength obtained by Voon [18] through prism tests. This base strength was multiplied by the respective factors to obtain the effective strengths of the members. The reinforcement yield strength was that reported by Voon [18] and any distributed applied axial load was resolved into equivalent point loads acting at the nodes across the top of each wall. The experimental strength used in the comparison was the average of the peak strengths from each of the two loading directions.

As the number of models for each wall type were developed, the errors between the results and the experimental strengths were inspected to identify patterns that could identify the source of each error. As potential sources of error were identified, variations from the ACI 318 code [8] modeling procedures were made to observe how they affected the modeling results in comparison with the experimental results. The adaptations that proved to consistently ameliorate the modeling results were adopted in the final modeling methodology.

The models were analyzed using MatLab [19]. The program consisted of functions that computed the parameters for each type of strut, a function that computed the strength for the entire model assembly, and a unique input file created for each specimen. The program used an iterative process to obtain each solution because there is no direct approach for solving all but the most rudimentary strut-and-tie models.

During the preliminary planning stages of the analysis, several types of strut geometries were identified to be common. These strut types were labeled according to the location of the known constraint locations at the top and bottom connections of the struts. Struts were classified as being in one of the following categories: center-to-edge, center-to-stirrup, edge-to-edge, and stirrup-to-edge. Illustrations of these four strut types are shown in Figure 3. Note that the center-to-center and edge-to-edge struts are very similar except for the definition of the distance d_s.

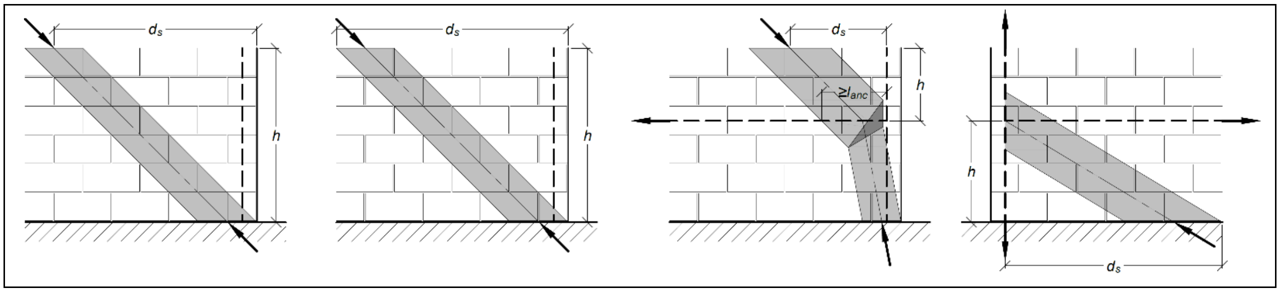

(a) Center-to-edge (b) Edge-to-edge (c) Center-to-stirrup (d) Stirrups-to-edge

Figure 3: Strut types

The first two strut types were sub-classified by whether or not their top anchorage extended into the header beam. This extension was based on the rigidity of the header beam in comparison with the masonry panel. A function was created for each strut type which calculated the size and resultant forces based on the given geometry, constraints, and applied force.

The main program used parameters from the input file to determine the geometry, constraints, and applied forces for each strut and passed those values to the appropriate strut-type function. The input parameters included the locations of the reinforcement, the grid points to which each strut was connected, the type of each strut, values for the various strut and node factors, and material properties. The program kept track of the stresses in the reinforcing bars and struts and adjusted the forces applied to the struts to ensure that the capacity of every member was not exceeded and that the model was in equilibrium. The main program summed the lateral contribution of all struts terminating in the base of the wall and output that value as the shear strength of the wall.

The layout and optimization of the models was performed manually by making changes to the input file for each specimen. This manual approach helped the analyst to observe how different perturbations to the models affected the resulting strengths. The program was updated throughout the study to accommodate the various adaptations that were developed specifically for the modeling of masonry shear walls.

Compression Struts

The effective compressive strength used for the masonry struts is given by Equation 2.

$$f'_s = 0.8\, \beta_s\, \beta_\alpha\, f'_m \qquad (2)$$

where β_s is the strut efficiency factor and β_α is the strut inclination factor.

Equation 2 is similar to that specified in ACI 318 code [8] except that the 0.85 factor for concrete was changed to 0.8 to maintain compatibility with other masonry strength equations and the strut inclination factor is introduced to account for the anisotropic behavior of masonry.

The strut efficiency factor β_s values from the ACI 318 code [8] were initially chosen as a baseline for the development of strut-and-tie models for the masonry specimens analyzed in this study. Struts that traveled in a near vertical direction near the edge of the wall were assumed to have a β_s value of 1.0 because the propinquity of the strut to the edge would prevent the stress fields from bulging. The struts that traversed the wall panels diagonally were assigned either a β_s value of 0.75 if they crossed at least one horizontal or vertical reinforcing bar or a value of 0.60 if they did not cross a reinforcing bar. During the course of the analysis, the values of β_s from ACI 318 code [8] also worked for the masonry models and at no time was there sufficient cause found to change the factor values from those initially selected. Further investigation and validation of β_s for use with masonry will require a test matrix of specimen groups each with similar strut layouts but varying levels of reinforcement and material strengths. Until further validation of strut efficiency factors can be performed with isolated specimens, the current values from the ACI 318 code [8] code have been observed to be suitable for use with masonry.

The strut inclination factor β_α values used in this analysis were chosen based on the theoretical strength curve developed by Liu et al. [20] for uniaxial masonry strength. The values for β_α were assumed to follow a bilinear approximation of the theoretical curve which gradually decreased from a value of 1.0 at a strut inclination of 0° to a value of 2/3 for 35°, after which the value was fixed at 2/3 as shown in Figure 4.

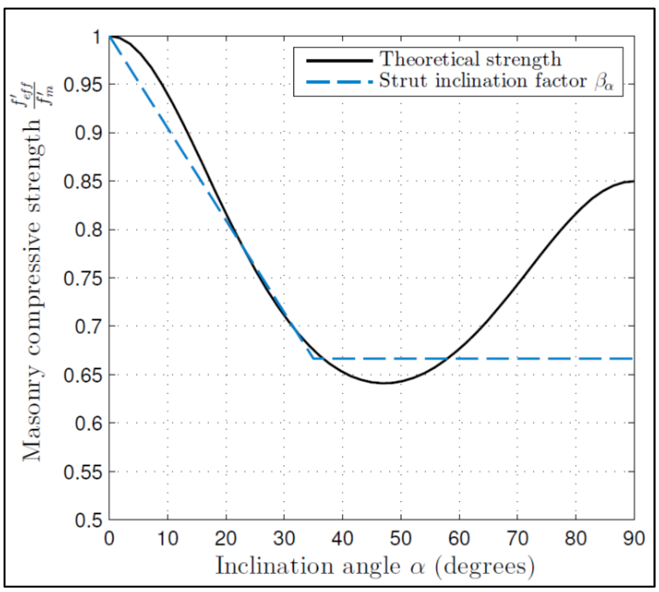

Figure 4: Strut inclination factor (Adapted from Liu et al. [20])

Nodal Zones

The effective strength of nodal regions was assumed to be given by Equation 3.

$$f'_n = 0.8\, \beta_n f'_m \tag{3}$$

where β_n is the node efficiency factor. The node efficiency factor was initially assumed to follow the provisions in ACI 318 code [8], which prescribe a value of 0.80 for nodal zones anchoring one tie and a value of 0.60 for nodal zones anchoring two ties. During the course of the analysis, no reason was found to justify any adjustment to the values initially selected.

The shear walls were all affixed to a reinforced concrete beam at their bases and to a steel channel at their tops. It was assumed that the base and steel channel were rigid bodies into which the struts could extend and in which the struts were anchored sufficiently. It was also assumed that the compressive and shear strengths along the wall-base and wall-header interfaces were at least as strong as the strengths of the bed joints within the wall panel. These two assumptions enabled the struts to transfer forces into the base or header at diagonal angles (in addition to vertically), negating the need for nodal zones within the masonry panel at the ends of some of the struts to redirect the forces in a vertical direction, as shown in Figure 5. The omission of nodal zones at the corners of the wall panel, along with their anchorage requirements, permitted the path of the strut from the wall panel directly into the header or base to extend clear to the edge of the wall panel, increasing the horizontal length and force contribution of the strut. It was observed, during the analysis, that these two assumptions appeared to be valid in the case of masonry shear walls.

(a) Deformable base (b) Rigid base

Figure 5: Strut boundary conditions at wall base

The reinforcement anchorage requirements used in the strut-and-tie models were assumed to follow those in the ACI 318 code [8] except that the equation for development length was taken instead from the TMS 402 code [21]. There were three types of anchorage identified. The first anchorage type was located within the header beam, and the vertical bars were assumed to be fully developed. In the second anchorage type, the lateral location of the nodal zone was governed by the width of the compressive struts and the development length of the stirrup, as shown in Figure 6(a). Since the stirrup was always hooked around the flexural reinforcing bar with a 180° hook, the development length equal to 13 (stirrup) bar diameters was used. The majority of the lateral force component from the diagonal strut was transferred to the stirrup while all of the vertical force component was transferred downward to a vertical strut. The strength of the stirrup was sometimes the limiting factor for the size of the diagonal strut. The last anchorage type differed from the second because it consisted of two perpendicular ties and a single strut, as shown in Figure 6(b). The AASHTO [10] provisions permit struts to extend up to six flexural bar diameters to either side of the stirrup when the stirrup is anchored to the flexural bar. In this scenario, the AASHTO [10] permits the flexural bar to provide full anchorage to the stirrup and strut and development lengths do not need to be checked. The strut width permitted by this provision was generally sufficiently large to transfer the full capacity of the stirrup if needed.

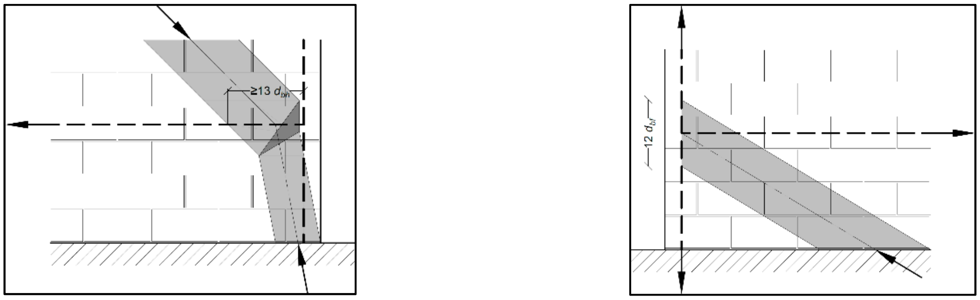

(a) Second anchorage type (b) Third anchorage type

Figure 6: Stirrup Anchorage Types

RESULTS

The results of the strut-and-tie models, with and without the strut efficiency factor, are summarized in Table 1. Also shown in Table 1 are the predicted strengths using the TMS 402 [21] shear equation. The fit of the strut-and-tie model predictions showed a lower coefficient of variation than the TMS shear equation, suggesting that strut-and-tie models are better at accounting for the variation in the wall geometry. The TMS equation results showed to be unconservative.

Table 1: Strut-and-Tie Models for Fully-Grouted Walls

Speci-men	Ultimate Shear Load (kN)			Strut-and-Tie Models				TMS 402 Equation	
				Including β_α		Excluding β_α			
	Min	Max	Avg	V_n (kN)	V_{exp}/V_n	V_n (kN)	V_{exp}/V_n	V_n (kN)	V_{exp}/V_n
A1	205	215	210	183	1.15	194	1.08	235	0.89
A2	177	195	186	187	0.99	205	0.91	219	0.85
A4	201	233	217	203	1.07	215	1.01	237	0.92
A7	261	263	262	229	1.14	245	1.07	274	0.96
A8	244	250	247	212	1.17	225	1.10	258	0.96
A9	204	207	206	156	1.32	172	1.19	288	0.71
A10	572	598	585	578	1.01	622	0.94	596	0.98
				Mean	1.12	**Mean**	1.04	**Mean**	0.90
				COV	0.100	**COV**	0.093	**COV**	0.105

The predictions for the strut-and-tie models analyzed in this study outperformed those of the TMS shear equation. In the case of specimen A9, the strut-and-tie model predicted a value that deviated more from the experimental results than that of the other specimens. Comparison of the experimental-to-predicted strength ratios for specimen A9 revealed that the lack of accuracy was similarly observed for the prediction using the TMS shear equation and that the specimen could possibly be labeled as an outlier because it did not perform as would be expected. The disparities between the experimental and predicted values in this case could be a result of measurement errors in the material or other wall parameters reported in the literature. It appears that the ability of the strut-and-tie models to consider the subtle differences in reinforcement placement and wall geometry make them more precise at describing and predicting the shear behavior of masonry walls that the shear equation. The improved precision of the strut-and-tie modeling method comes at the expense of requiring more effort and understanding on the part of the designer.

DISCUSSION

The construction of strut-and-tie models for simple masonry shears walls showed that the process is straightforward and can be mastered quickly with some practice due to the typical geometry of masonry shear walls. The most important principles of creating strut-and-tie models are that all forces and reactions be in equilibrium, the design strength of all members meet or exceed the ultimate factored load applied to them, and that the geometry of all members be considered in determining their layout, loading, and strength.

All loads and reactions applied to the masonry shear wall must be in equilibrium to prevent rigid-body translation or rotation of the model. Loads and reactions, including distributed loads must be applied to the model at nodes. Distributed load must be resolved into equivalent point loads based on the principles of tributary area and static equilibrium. Without these two principles there would be nothing to prevent the designer from assuming that the entire distributed load acts at the point that would produce the greatest lateral force component. Models must have a path for the entire axial load to traverse the wall from the top to bottom; so it is generally best to first model the struts to indicate the path of the axial load to the ground. Once the model has been laid out for the axial load component, the strut widths can be increased to account for the additional vertical forces contributed by the vertical reinforcement.

Plasticity theory assumes that stresses have already been redistributed to other members within the wall due to yielding and cracking, meaning that strut-and-tie models already account for much of the redundancy from the indeterminate geometry of the wall. Due to the relatively small number of members in a strut-and-tie model and the weakest link theory, failure of any single member in a strut-and-tie model would typically result in a reduction in peak strength capacity for the entire wall. The corollary to this requirement is that the members—particularly the reinforcement and nodes—do not have to be fully stressed to their capacity in the final model.

Attempting to use the full strength of the reinforcing bars can result in a model with a less-than-optimum strength capacity or an infeasible model. This is because the struts traversing the wall diagonally contribute the most to the lateral capacity of the wall. The inclination of the diagonal struts was determined to be heavily influenced by the less-inclined strut that terminated in the toe between the diagonal strut and the edge. As the width of the less-inclined strut increased, it pushed the terminus of the diagonal strut farther from the leading edge, reducing the diagonal strut’s inclination and its lateral force component. The increase in the lateral strength component of the less-inclined strut was frequently less than the loss in strength by the diagonal strut, resulting in an overall decrease in the wall shear capacity.

The geometry of the struts, ties, and nodes must be considered in determining the layout of the model, the loading applied to each member, and the strength capacity of each member. This principle is the foremost difference between the full strut-and-tie modeling procedure and the equivalent-truss modeling procedure used by some researchers for reinforced masonry shear walls. The greatest impact to the layout of the struts is caused by the requirement for sufficient reinforcement anchorage and the ordering of struts in the compression toe of the wall.

SUMMARY OF THE ANALYSIS PROCEDURE

The procedures for constructing strut-and-tie models for masonry shear walls is as follow:

1. Resolve the distributed axial load into point loads acting along the center lines of the nodes located at the tops of the vertical reinforcing bars. Divide the distributed load according to the tributary area of each node assuming that the shear wall thickness is constant.

2. Layout struts from the nodes to the compression toe of the wall, incorporating the usage of horizontal reinforcing bars. Each strut should enter the toe sequentially and be placed such that no two struts overlap. The thickness of each strut should be calculated beginning with the leading-most strut and working backwards toward the trailing strut. Once the thickness of a strut has been determined, the toes of the struts behind it are moved such that they touch but do not intersect.

3. After the model is in equilibrium for the exterior applied forces, add in the contribution of the vertical reinforcement beginning with the trailing-most vertical bar and working toward the leading-most bar. As the contribution increases the applied force to the corresponding strut, the strut width must be increased so that the strut strength is equal to the force applied to it. As the strut widths change, the strut paths must be adjusted so that they do not encroach into one another.

4. When the trailing end of a horizontal reinforcing bar is anchored to a vertical bar, the vertical component of the descending strut must be subtracted from the contribution of the bar at its top.

5. The model is complete when the forces are in equilibrium, the strength of all materials are less than the applied forces, the anchorage requirements are met, no two struts cross or overlap, and the model strength is maximum.

SUMMARY

While the proposed methodology is preliminary and still imperfect, the results of this analysis have shown that strut-and-tie model guidelines based on the methodology originally proposed by Schlaich et al. [7] for reinforced concrete are valid for masonry design with minor adaptations. The shear strength predictions from the proposed strut-and-tie modeling methodology were shown to out-perform those of the shear strength equation. It has been observed that the vertical reinforcement nearest the trailing edge of the wall and the horizontal reinforcement in the middle half of the wall are most effective in contributing to the shear capacity of masonry shear walls.

REFERENCES

[1] Ganz, H. R. and Thürlimann, B. (1983). "Strength of brick walls under normal and shear forces." *Proc. of the 8th International Symposium on Load-Bearing Brickwork*, 27–29. London.

[2] Mojsilovic′ N, Marti P. (1997). "Strength of masonry subjected to combined actions." *ACI Struct J.,* 94(6), 633–42.

[3] Mojsilović, N., Kostić, N., and Schwartz, J. (2013). "Modelling of the behaviour of seismically strengthened masonry walls subjected to cyclic in-plane shear." *Engineering Structures*, 56, 1117–1129.

[4] Bower, A. F. (2011). *Applied mechanics of solids*. CRC Press, Boca Raton, FL. (Available online at: http://solidmechanics.org/).

[5] Collins, M. P. and Mi (1988). "Shear and torsion design of prestressed and non-prestressed concrete beams." *J. of the Prestressed Concrete Institute*, 25(5), 32–100.

[6] Marti, P. (1985). "Basic tools of reinforced concrete beam design." *ACI Journal*, Proceedings, 821, 45–56.

[7] Schlaich, J., Schäfer, K., and Jennewein, M. (1987). "Toward a consistent design of structural concrete." *J. of the Prestressed Concrete Institute*, 32(3), 74–150.

[8] ACI 318 (2011). *Building Code Requirements for Structural Concrete (ACI 318-02) and Commentary (ACI 318R-02)*. American Concrete Institute (ACI), Farmington Hills, MI.

[9] ACI-ASCE (1988). "Building code requirements for masonry structures (ACI 530–88, and ASCE 5–88)."

[10] AASHTO (2012). *LRFD Bridge Design Specifications*. American Association of State Highway and Transportation Officials (AASHTO), Washington.

[11] Liang, Q. Q., Uy, B., and Steven, G. P. (2002). "Performance-based optimization for strut-tie modeling of structural concrete." *J. of Structural Engineering*, 128(6), 815–823.

[12] Mojsilovic′, N. (2011). "Strength of masonry subjected to in-plane loading: A contribution." *International Journal of Solids and Structures*, 48, 865–873.

[13] Nolph, S. M. (2010). *In–Plane Shear Performance of Partially Grouted Masonry Shear Walls*. Master's thesis, Washington State University, Pullman, WA.

[14] Roca, P., Viviescas, A., Lobato, M., Diaz, C., and Serra, I. (2011). "Capacity of shear walls by simple equilibrium models." *International Journal of Architectural Heritage*, 5(4-5), 229–238.

[15] Varshney, A. (2010). *Simplified Analysis of Strength of Masonry Shear Walls*. Master's thesis, Universitat Politècnica de Catalunya, Barcelona.

[16] Voon, K. C. and Ingham, J. M. (2006). "Experimental in-plane shear strength investigation of reinforced concrete masonry walls." *J. of Structural Engineering*, 132(3), 400–408.

[17] Voon, K. C. and Ingham, J. M. (2008). "Experimental in-plane investigation of reinforced concrete masonry walls with openings." *J. of Structural Engineering*, 134(5), 758–768.

[18] Voon, K. C. (2007). *In–Plane Seismic Design of Concrete Masonry Structures*. Ph.D. thesis, University of Auckland, Auckland.

[19] MatLab (2014). MatLab R2014a. MathWorks, Natick, MA.

[20] Liu, L., Tang, D., and Zhai, X. (2006). "Failure criteria for grouted concrete block masonry under biaxial compression." *Advances in Structural Engineering*, 9(2), 229–239.

[21] MSJC (2013). *Building Code Requirements for Masonry Structures (TMS 402–13, ACI 530–13, and ASCE 5–13)*. The Masonry Society, American Concrete Institute, and ASCE; Boulder, CO; Farmington Hills, MI; and Reston, VA.